

Tracing and Mitigating Virus Diffusion via a Fine-Grained Timeline Contact Graph

Yipeng Zhang, Zhifeng Bao
RMIT University
Melbourne, Australia
yipeng.zhang,zhifeng.bao@rmit.edu.au

Yuchen Li, Baihua Zheng
Singapore Management University
Singapore
yuchenli,bhzheng@smu.edu.sg

Xiaoli Wang
Xiamen University
Xiamen, China
xlwang@xmu.edu.cn

Abstract—In this work, we aim to achieve two goals: (1) how to accurately and efficiently model the virus diffusion according to fine-grained users’ movement records, and (2) how to help the government evaluate the effectiveness of different checkpoint deployment strategies to mitigate virus diffusion. For concreteness, we use the public transport system as a scenario for illustration. We associate the virus with two parameters, *incubation period* and *transmissibility*, which simulate how fast the virus could be spread and hence determine how dangerous it is. To accurately model virus diffusion, we propose a diffusion model based on a new data structure namely *timeline contact graph* (TCG), which essentially is a weighted directed graph $G = (V, E)$. Here, $v \in V$ is a trip record of a passenger, and $e \in E$ from nodes v to v' indicates the virus infection from v to v' , and the weight of e is the infection probability. TCG is able to record all close contacts when there are boarding/alighting passengers. In addition, we formulate two problems, Epidemic Mitigating in Public Area problem (*EMA*) and Epidemic Maximized Spread in Public Area problem (*ESA*). *EMA* is to find an ideal checkpoint deployment strategy; *ESA* is to find a set of ‘super-spreaders’ to simulate an extreme case that the virus is spread widely, which then help to test the robustness of checkpoint deployment strategies. Finally, we conduct experiments using real-world station datasets and millions of public transport trip records to verify the usefulness and scalability of our approach.

Index Terms—Tracing, Virus Diffusion, Graph

I. INTRODUCTION

Plagues and epidemics have ravaged humanity since the birth of civilisation, often changing the course of history. As per the World Health Organization’s (WHO) guidance to government in managing epidemics [1–3], there are two essential measures, (1) *tracing close contacts*, and (2) *deploying checkpoints*, which have been widely applied worldwide [4–6]. In this work, following the guidance of controlling pandemic from WHO [1, 3], we plan to adopt a data-driven approach to model and help mitigate virus diffusion within the society. In what follows, we present the two main goals of our work, and then highlight the challenges before presenting our solutions.

Goal 1. Tracing Close Contacts in Short-term. In the COVID-19 pandemic, according to WHO [3], a close contact is a person who shares a space with an infected person for more than 15 minutes in the past 2 to 14 days, where the space can be the public or shared transport, places of worship, workplaces, schools, or private social events. It is urgent and necessary for the government to identify all close contacts who

have contacted infected persons. Therefore, our first goal is to exactly find all persons who are the most likely to be infected given the infection model within a *short-term* (e.g., 7-28 days). This also differentiates our work from a long list of existing work [7–16] on virus infection within a much longer term (e.g., a year or even longer) at the census of population level.

Goal 2. Deploying Checkpoints in Short-term. Deploying checkpoints to detect and quarantine infected persons, as an effective measurement, has been used extensively worldwide [4–6]. Hence, our second goal is twofold. First, we aim to find top- k locations for building checkpoints to detect infected persons and to minimize the risk of an outbreak within a short-term (e.g., 7-28 days). Second, we evaluate the effectiveness of different checkpoints deployment strategies from two perspectives (defense v.s. offense). From the defensive perspective, we formulate the problem of Epidemic Mitigating in Public Area (*EMA*) to find an ideal checkpoint deployment strategy such that virus diffusion can be well mitigated. From the offensive perspective, we introduce the Epidemic Maximized Spread in Public Area problem (*ESA*) to find k highly infectious persons and to evaluate the robustness of any given checkpoint deployment under the attack from k ‘super-spreaders’.

Challenge 1 – The first challenge is how to emulate the virus spread accurately. Specifically, there are two essential requirements: (1) The spread model has to consider the exposure duration when evaluating the infection probability among people. We have shown that the infection probability highly depends on the exposure duration [1–3]. (2) The temporal order of the contacts among persons is critical. For example, given two passengers taking the same bus, if one passenger boards the bus at a station while the other alights at the same station, they do not have a contact. To the best of our knowledge, most existing studies aim to find the pandemic threshold in a coarse-grained *long-term* simulation. Hence, they are unable to consider exposure duration and temporal order. We will further discuss their limitations in Section II-A.

Challenge 2 – The second challenge is how to address the high computational costs. The population of most metropolitan cities is at the scale of millions or even tens of millions. For example, in our dataset, four weeks of bus riding is at the scale of ten million records. For finding super spreaders and building checkpoints, neither an eigenvalue-based solution nor a Monte

Carlo simulation is practical due to the massive amounts of data. More details will be discussed in Section II-A.

Our Solutions. We introduce a virus diffusion model that offers a fine-grained and efficient measurement. In this model, a virus is associated with two parameters, the *incubation period* and the *transmissibility* [17, 18]. The former refers to the duration between when a person is infected and when she is able to infect others; the latter determines the likelihood of a healthy person getting infected by an infected person according to the exposure duration. It is worth noting that picking the right parameter values is not the focus of this paper, but rather we leave the settings to epidemic experts.

Our framework is based on a new data structure, *timeline contact graph* (TCG), to record all changes of close contacts when people change their locations, so that we can accurately evaluate the infection probability of each movement according to the contact time to address the first challenge. In order to find the ideal checkpoint deployment strategy for the *EMA* problem and the ‘super-spreaders’ for the *ESA* problem, we introduce the concept of *Contact Paths Tracing* (CPT), which allows us to efficiently find the high-risk movements that may infect a large number of persons without performing Monte Carlo simulations to tackle the second challenge.

In summary, our contributions include the following:

- We propose a novel Timeline Contact Graph (TCG), based on which we propose a diffusion model that can capture the connections between persons that are expected to change frequently (Section IV). It reduces the time-cost of modelling virus diffusion within a society.
- We formulate the Epidemic Mitigating in Public Area problem (*EMA*). To our best knowledge, this is the first work that studies the epidemic spread/mitigation based on real-world individual movement records. We prove the NP-hardness of *EMA* problem. We introduce the concept of Contact Paths Tracing (CPT) that indicates all risky movements of persons, and propose a CPT-based solution for *EMA* (Section V).
- We formulate the Epidemic Maximized Spread in Public Area problem (*ESA*). We also prove the NP-hardness of the *ESA* problem and propose an efficient method to address *ESA* based on CPT (Section VI).
- We conduct extensive experiments on real individuals’ movement records. We adopt the Susceptible Infected (SI) model. First, we compare our diffusion model based on the TCG and the dynamic graph with the different periods of snapshots in terms of efficiency and effectiveness in modelling the virus diffusion. Then, we test whether our solution for the *EMA* problem can find a proper checkpoint deployment strategy to mitigate the epidemic against the baseline. Last, given a checkpoint deployment strategy, we further test the impact of the different number of selected ‘super-spreaders’ as initially infected persons against a baseline (for the *ESA* problem) in controlling a potential outbreak (Section VII).

II. RELATED WORK

In this section, we introduce the most related work falling into two categories, *virus immunization* and *influence maximization*. We will mainly introduce virus immunization work since it is closer to our work, which aims to study the prevention and diffusion of the virus.

A. Virus Immunization

Virus Immunization (VI) studies how the virus diffuses and how to control the virus diffusion [19]. The three most common compartments in all epidemic models are Susceptible (*S*), Infected (*I*), and Recovered (*R*) [20–22]. *S* represents the set of people who are healthy but susceptible to be infected. *I* represents the set of people who are infected but are able to recover. *R* represents the set of people who are recovered already, but may be infected again based on different problem settings. Various models, such as SIS, SIRS, SEIR, and SEIRS, are defined in order to better accommodate the biological properties of real diseases [19, 23]. For instance, the SEIR model is a variation of the SIR model and it includes a stage of exposed (*E*) individuals, referring to persons who have been infected but cannot transmit the disease yet.

Our work is fundamentally different from most VI studies from the perspective of the virus model, the objectives, and the methodology, respectively, as illustrated below.

Objective: Most studies [7–11, 24–28] in VI focus on the question of “will the pandemic happen at long-term at *population-level*?” The difference is three-fold: time period, analytical granularity, and the goal. For instance, given a graph *G*, the *goal* of the work [28] is to find a threshold of the first eigenvalue λ^* , such that the virus will diminish when the time approaches infinity (*time period*) if λ of *G* is smaller than λ^* , otherwise it will become a pandemic. Each node in the graph represents a city (*analytical granularity*).

In contrast, our *goal* is to accurately track how the virus spreads through each person (*analytical granularity*) based on the close contacts within one month (*time period*). In other words, we answer the question of “Who will be infected?”

Virus Model: Since most VI works study the long-term trend of virus spreading, they consider the recovery phase and re-infection phase. Therefore, most of them are based on the SIS, SIRS, or SEIRS model. Conversely, our work targets a period of few weeks, where a person is unlikely to be healed and infected repeatedly. Therefore, we adopt the SI model.

Methodology: Existing VI studies fall into two categories, based on either the betweenness centrality [12–14] or the eigenvalues [15, 16]. In a nutshell, the core idea behind these two classes of solutions is to remove the node/edge that has the highest centrality or can maximally decrease the first eigenvalue of the graph. However, those existing solutions suffer from two common drawbacks.

First, it has been shown that the time-varying connectivity pattern of networks will affect the epidemic process in numerous ways [19, 23], while most of the above studies utilize a fixed graph. For a few studies based on a varying graph or temporal graph, a common approach for VI problems

is to utilize the snapshots corresponding to different time intervals [16, 29–31], which causes the accuracy and efficiency issues, to be detailed in Section IV-A. To name a few, in the work [16], given N snapshots, it first evaluates the drop of the eigenvalue of removing each node for each snapshot and then, at each step, it removes the node that causes the largest drop of the average eigenvalue among all snapshot-based solutions. Second, to the best of our knowledge, none of the existing works fully utilizes spatial-temporal movement records to model and prevent the virus diffusion. As mentioned in Section I, the spatial and temporal properties of contacts based on the movement records are critical to model the virus diffusion as the two essential components of virus infection are *close contacts* that are spatial-location dependent and *exposure duration* that is temporal dependent [3].

B. Influence Maximization

The Influence Maximization (IM) problem aims to select a k -sized seed set in an online social network to maximize the expected number of influenced people through the seed set in information diffusion, which is similar to the ESA problem. There are a few existing studies that take the varying connections of nodes into account. The Time-Constrained IM problem [32] introduces a Latency-Aware Independent Cascade model to compute the influence between two persons, where the influence equals the product of influence probability and the delay probability. In the Continuously-activated and Time-restricted Independent Cascade (IC) model [33], each active node can activate its neighbors repeatedly until a given deadline. Given that a social network is constantly evolving and important users with the most influence also change over time, the authors in [34] try to identify a seed set that can influence the largest number of distinct users over a predefined window of time. To the best of our knowledge, no existing work uses spatial-temporal movement to model the virus diffusion, whereas in our work, the infection probability is based on physical contacts and exposure duration among people. Therefore, the IC model is insufficient as a predictive model for tracing virus spread.

III. PRELIMINARIES

In this work, we have two goals: (1) how to accurately and efficiently model the virus diffusion according to fine-grained user movement records, and (2) how to help the government evaluate the effectiveness of different checkpoint deployment strategies to mitigate virus diffusion. In the following, we first present how to measure the infectious probability between persons (for Goal 1); we then formulate the problems of *ESA* and *EMA* (for Goal 2). Table I lists important notations that will be used frequently in the paper.

A. Notations

Check-in. Given a check-in database \mathcal{T} , a check-in record $tr_i \in \mathcal{T}$ is a tuple $\{s, t_b, t_e\}$, where s denotes a check-in point of interest (POI), while t_b and t_e denote the check-in time and check-out time, respectively.

TABLE I: Important notations

| Notation | Description |
|----------|---|
| γ | Incubation threshold |
| p_n^i | The i -th check-in record of p_n , $p_n^i \in p_n.Tr$ |
| $R()$ | The duration of exposure of one contact |
| $f()$ | Infection probability measurement based on $R()$ |
| $I(P)$ | Infection range, the set of people infected by p |
| $W(S)$ | Coverage width, the set of check-ins covered by S |

TABLE II: Timetable of check-in records

| | Day 1 | | Day 2 | |
|---------------|---------------|-------------------|---------------|-------------------|
| \mathcal{P} | \mathcal{T} | Check-in & out | \mathcal{T} | Check-in & out |
| p_1 | tr_1 | 8:06:28 - 8:15:45 | tr_2 | 8:01:56 - 8:16:32 |
| p_2 | tr_1 | 8:01:12 - 8:15:45 | tr_2 | 8:01:56 - 8:16:32 |
| p_3 | tr_1 | 8:01:12 - 8:06:28 | tr_2 | 8:01:56 - 8:07:11 |

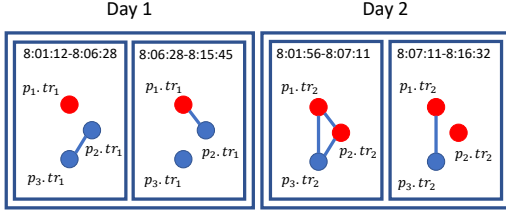
Person. Given a person database \mathcal{P} , each person $p_n \in \mathcal{P}$ has a set of check-in records $p_n.Tr = \{tr_i, \dots, tr_j\}$. Let p_n^i denote the check-in record tr_i of p_n . A person is in either a healthy state ($p_n = 0$) or an infected state ($p_n = 1$).

B. Infection probability

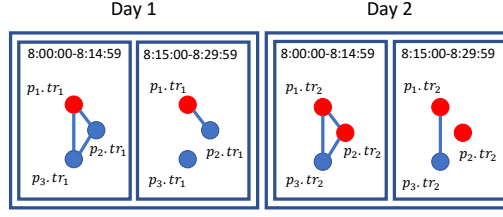
The infection probability refers to the risk of a healthy person getting infected by an infected person when they have a contact. Existing studies [17, 18] have shown that a longer exposure duration between persons leads to a higher infection probability. We follow this finding and utilize two types of well-known infectious probability measurements. Let $Pr(p_n^i, p_m^j) = f(R(p_n^i, p_m^j))$ be the infection probability between two persons after one contact (i.e., contact between i -th check-in of p_n and j -th check-in of p_m). Here, $R()$ is the exposure duration of one contact, defined as $R(p_n^i, p_m^j) = \max((\min(tr_i.t_e, tr_j.t_e) - \max(tr_i.t_b, tr_j.t_b)), 0)$ if $tr_i.s = tr_j.s$, and $R(p_n^i, p_m^j) = 0$ otherwise; $f()$ measures the infection probability based on the exposure duration. The two measurements that we utilize cover continuous and discrete models. The first one, EC_{50} , is a non-linear model [35], in which the infection probability increases when the duration increases. The second one is a binary model; given a threshold, $f() = 100\%$ if $R()$ is longer than the threshold, and 0% otherwise. More details will be presented in Section VII.

Subsequently, we have the probability of a person being infected after a check-in record, which is $Pr(p_n^i) = 1 - \prod_{tr_j \in (\mathcal{T} \setminus p_n.Tr)} (1 - Pr(p_n^i, p_m^j))$. Intuitively, it equals one minus the probability of avoiding being infected from all close contacts after having the check-in $p_n.tr_i$. Consequently, the probability that a person p_n will be infected (by considering all the check-in records that p_n has made) is defined as $Pr(p_n) = 1 - \prod_{tr_i \in p_n.Tr} (1 - Pr(p_n^i))$.

Example 1. We use Figure 1b as an example to present how to measure the infected probability. For concreteness, we quantify the infection probability based on the EC_{50} model, $f(R) = 1/(1 + (EC_{50}/R)^\tau)$. We set $EC_{50} = 800$ seconds and $\tau = 5$. Under this setting, $Pr(p_n^i, p_m^j) = 50\%$ when $R(p_n^i, p_m^j) = 800$ seconds. Given a check-in record database \mathcal{T} as listed in Table II, where $p_1.Tr = \{tr_1, tr_2\}$,



(a) Correct close contact relationship



(b) Snapshot updates every 15 minutes

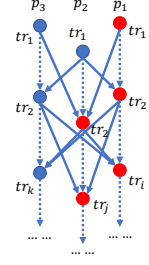


Fig. 2: Timeline Contact Graph (TCG) based on Table II

Fig. 1: The two figures show two dynamic graphs. Each node is a check-in of one person. The red node indicates that this person is infected during this check-in, whereas blue indicates the healthy status. The edge connects two trips if the trips are close contact.

$p_2.Tr = \{tr_1, tr_2\}$ and $p_3.Tr = \{tr_1, tr_2\}$, we have $Pr(p_2^1, p_1^1) = 1/(1 + (800/557)^5) = 14\%$, and $Pr(p_2^1, p_3^1) = 1\%$. Subsequently, $Pr(p_2^1) = 1 - (1 - 14\%)(1 - 1\%) = 14.86\%$. Similarly, we have $Pr(p_2^2) = 64.79\%$. Consequently, after day 2, the probability of p_2 getting infected is $Pr(p_2) = 70.02\%$.

C. Incubation Period.

When a person is infected, she/he is not able to infect other healthy persons immediately because of the incubation period. We define the incubation period as γ hours. For instance, if p_n is infected at the check-in record tr_i , then p_n will be infectious and detectable from $tr_i.tb + \gamma$ onward, i.e., γ hours after tr_i .

Now, based on the infection probability and incubation period, we are able to simulate the virus spread. Let $I(p_n^i)$ denote the set of people who will be infected by p_n^i . Accordingly, $I(p_n) = \cup_{tr_i \in p_n} I(p_n^i)$ denotes the set of people who will be infected by $p_n \in P$. Then, we have $\cup_{p_i \in P} I(p_i)$, the set of people who will be infected by P . Consequently, we have $I_{P,T,\gamma}(P) = |\cup_{p_i \in P} I(p_i)| = \mathbb{E}[\sum_{p_n \in P} Pr(p_n)]$, which is the expected number of infected people caused by P .

IV. MODELING THE VIRUS DIFFUSION

As highlighted in Section I, a major challenge faced by this study is how to model the virus diffusion accurately and efficiently, given the dynamic nature of the contacts between persons that are ever-changing when persons are accessing and leaving different POIs, i.e., a dynamic infectious graph. In what follows, we first introduce the drawbacks of employing existing works in dealing with the dynamic infectious graph; we then introduce a novel graph structure, namely Timeline Contact Graph (TCG), to address this challenge; we finally explain how to model virus diffusion based on TCG.

A. Pain Points

Recall Section II-A, most, if not all, existing studies utilize snapshots to capture the changing contacts between persons [16, 29–31, 36, 37]. For example, they generate multiple snapshots based on some criteria to record the state of graph containing all edges and vertexes. Taking our problem as an example, each node in a snapshot represents a person, and an edge between two persons denotes the infection probability between them. Once the graph changes, including

adding/deleting nodes/edges, a snapshot has to be generated to record the current graph before the change. However, the snapshot-based solutions suffer from either the efficiency issue or the accuracy issue.

Accuracy Issue. The snapshot-based solutions may overlook the *fine-grained temporal order* of contacts between persons. We use the following example to explain the importance of the temporal order of contacts in real-world check-in records.

Example 2. Continuing the setting in Table II, Figure 1b presents how the dynamic graph with snapshots for every 15 minutes captures the contacts between persons. Since p_1 , p_2 and p_3 are at the same POI from 8:00:00 to 8:14:59 on day 1 (i.e., they are connected to each other in the first snapshot of Figure 1b), they can infect each other. However, it is incorrect because the moment p_1 checks-in this POI, p_3 checks-out the POI. Consequently, p_1 cannot infect p_3 on day 1, which contradicts the facts captured by the first snapshot. The correct contact relationship is shown in Figure 1a.

Efficiency Issue. As shown in Example 2, low update frequency cannot capture the correct close contact relationship. However, if we generate a snapshot in a very short interval (e.g., 10 seconds), it will be unaffordable to any existing solution, due to a massive amount of snapshots. For example, a recent work [15] prevents virus diffusion by removing nodes based on the first eigenvalue; the experimental result shows that removing 50 nodes on one graph that has 13,947 nodes and 61,168 edges will take more than 4,000 seconds.

B. Timeline Contact Graph (TCG)

In order to address the above issues, we propose TCG that is able to capture all the contacts between records. Essentially, in this graph, a vertex is not a person, but a record.

Definition 1. *Timeline Contact Graph:* A TCG is an ordered pair $G = (V, E)$, where V is a set of vertices, with each representing a record $tr_i \in \mathcal{T}$, and $E = \{\{v_i, v_j\} | v_i, v_j \in V \text{ and } v_i \neq v_j\}$ is a set of edges, with each edge $v_i \rightarrow v_j$ representing the infection probability from v_i to v_j , i.e., $e = \{v_i, v_j\} = Pr(p_n^i, p_m^j)$.

There are two different types of edges, the *self-infection edge* and the *infection edge* between different persons. The

former is to connect a record made by a person to her next record based on the temporal order of the check-in time. We assume self-infection is 100%. The latter is to connect a record tr_j made by person p_m to another record tr_i made by a different person p_n , if $Pr(p_n^i, p_m^j) > 0$. As shown in Figure 2, dotted lines refer to self-infection edges and solid lines refer to infection edges between different persons.

Based on the TCG, we can easily model the virus diffusion when the contacts are frequently changing. In our problem, since we only focus on precisely modeling the virus infection in the individual-level for a short period (i.e., 7-28 days) instead of simulating the virus trend in the population-level for a long time, we do not consider the recovery and reinfection case. Therefore, we use the widely adopted Susceptible-Infected (SI) model [20, 22] as a virus diffusion model. In each record, an infected person has a probability to infect all neighbors through the outgoing edges independently with the edge weights indicating the infection probabilities.

C. Infection Propagation

When an infected person p_n is making a check-in tr_i , p_n will attempt to infect other persons p_m under the probability $Pr(p_n^i, p_m^j)$. We describe the following routine to simulate the infection propagation process.

1. We initialize an empty priority queue of check-in records, with all the records sorted based on an ascending order of the check-in time.
2. Given a set P of persons who are initially infected, we assume the remaining persons (i.e., $\mathcal{P} - P$) are healthy. We push the first trips of all the infected persons (i.e., $\cup_{p_n \in P} p_n^1$) into the queue.
3. The queue pops a record tr_i iteratively. While checking in a POI via tr_i , p_n infects other persons in the same POI with a probability $Pr(p_n^i, p_m^j)$.
4. We push all check-in records that have not been infected but will be infected by tr_i into the queue.
5. Repeat steps 3 and 4 until the queue is empty.

Example 3. This example is based on Table II. For initialization, we set the incubation period as 12 hours, and set p_1 to be infected and push p_1^1 into the queue, while both p_2 and p_3 are healthy. First, we pop p_1^1 , and calculate the infection probability from tr_1 with all contacts. Assume p_2 is infected after p_1^1 , due to the incubation, p_2 is infected at 20:01:12. Subsequently, we push p_2^2 into the queue. In addition, p_1^2 will be infected by p_1^1 with 100% as it is a self-infection.

V. EPIDEMIC MITIGATING IN PUBLIC AREA

As mentioned in Section I, our second goal is to evaluate the effectiveness of different checkpoint deployment strategies from two different perspectives (defense v.s. offense). In this section, from the defensive perspective, we study the problem of Epidemic Mitigating in Public Area (EMA), in order to find an ideal checkpoint deployment strategy such that virus diffusion can be well mitigated.

Noting that, it is almost infeasible to accurately estimate the number of infected persons in practice [38–42]. This

implies that the measures of controlling pandemics are usually operated without knowing the *exact* picture of the disease. Therefore, we study a more challenging yet practical problem for policy-makers: how to maximize the coverage of checkpoints? Essentially, the coverage of a POI is evaluated by the “vulnerability”, that is, if infected persons arrive at this POI, how many persons would be infected.

In the following, we first introduce the problem definition of EMA and prove that EMA is NP-hard. Next, based on the novel structure TCG, we propose a concept called *Contact Paths Tracing (CPT)* that is generated based on the latest check-in record of a person p_n . It presents a set of contacts that have the potential to infect the person p_n . Last, we propose our solution to address the EMA problem based on CPT.

A. Problem Definition of EMA

The motivation of EMA is that, if we could detect that p_1 is infected before she accesses a POI, we could stop p_1 from accessing a POI and infecting other persons in the same POI, and meanwhile quarantine p_1 from spreading the virus in the following days. To implement the above idea to block the diffusion of the virus, we introduce a checkpoint corresponding to a POI, which allows us to implement certain measures (e.g., new cutting-edge rapid tests are able to detect COVID-19 in a few minutes [43–45]) and to find all potentially infected persons when they are accessing POIs.

Definition 2. *Checkpoint:* Given a POI s and a person p_n who makes a check-in tr_i at s , if s is set as a checkpoint, p_n is allowed to check-in and check-out if she is healthy and meanwhile passes the screening test implemented at s ; p_n will be isolated if she is infected (and accordingly, $p_n.Tr = \{tr_i, \dots, tr_{|Tr|}\}$ are removed from \mathcal{T}).

Recall that $I(p_n^i)$, introduced in Section III-C, denotes the set of persons who will be infected by p_n^i (i.e., have contacts with p_n during tr_j). Let $W(tr_i) = I(p_n^i)$. Accordingly, we define a new metric $W(s_n)$ to denote the coverage of the checkpoint s_n below, where ∂s_n refers to a set of check-in records such that $\forall tr_i \in \partial s_n, tr_i.s = s_n$. Consequently, we have $W(s_n) = \cup_{tr_i \in \partial s_n} W(tr_i)$. We are now ready to formally present the problem definition for EMA.

Definition 3. *EMA problem:* Given a person dataset \mathcal{P} , a check-in record dataset \mathcal{T} , a checkpoint candidates dataset S , a budget k , and an incubation threshold γ , EMA is to find a set of POIs $S \subseteq \mathcal{S}$ to set up checkpoints so as to maximize the coverage of checkpoints.

$$S = \operatorname{argmax}_{|S| \leq k} W_{\mathcal{P}, \mathcal{T}, \gamma}^*(S) = |\cup_{s_i \in S} W(s_i)|. \quad (1)$$

A straightforward solution is to select the top- k POIs that have the largest number of check-in records. However, a POI with a larger number of check-in records is not necessarily a POI having a higher vulnerability. For example, considering a POI with many check-in records that come from a fixed crowd with a constant movement pattern, where another POI with fewer check-in records from a group of highly mobile

persons. Clearly, the latter POI is more vulnerable. The experimental results to be reported in Section VII-F also confirm this observation. As compared to the checkpoint deployment strategy that always picks the top- k POIs (based on the volume of check-in records), our solution can improve the coverage by at most three times.

Theoretically speaking, an optimal checkpoint deployment strategy should be able to well mitigate the virus from spreading among all situations, which is equivalent to minimizing the maximum number of finally infected persons no matter who the initially infected persons are [46, 47]. However, to the best of our knowledge, there is no existing work that could be applied to address our problem because of two main reasons: (1) They do not consider a varying graph as a result of persons' movements. (2) The scale of the people/check-in records considered by existing work is significantly smaller than that considered in our problem, and hence all existing works cannot be a solution to our problem because of efficiency issue. For instance, existing work [47] proposes a dynamic index data structure (WC) designed for influence analysis when some of edges or nodes are removed from the graph. With the dataset that is one order of magnitude smaller (Flickr (WC) 2.2×10^6 nodes, 2.3×10^7 edges; EZ-LINK (Our work) 1.3×10^7 nodes, 1×10^8 edges), WC needs more than 4,000 seconds to build the dynamic index data structure, and needs to update the index after removing edges/nodes in each iteration. In contrast, our solution costs less than 300 seconds in the default settings for finding 50 POIs to build checkpoints.

B. Hardness of EMA

Theorem 1. *The EMA problem is NP-hard.*

Proof. We prove it by reducing the Minimum k -union Problem (MinKU) [48]. In the MinKU problem, given a collection of set $S' = \{s'_1, s'_2, \dots, s'_m\}$ where each set s'_i is a subset of a given ground set \mathcal{P}' , an integer $0 \leq k \leq m$ and $0 \leq \tau \leq |\mathcal{P}'|$, it aims to find $S' \subseteq S'$, such that $|S'| = k$ and $|\cup_{s'_i \in S'} s'_i| \leq \tau$. We map the MinKU problem to the EMA problem with the following process: (1) In EMA problem, let each person has two check-ins only; let $\gamma = 0$; let $f(R()) = 100\%$ if $R() > 0$. (2) We map each check-in p in EMA to each element $p' \in \mathcal{P}'$ in MinKU, and map each candidate location $s \in \mathcal{S}$ in EMA to each set $s' \in S'$ in MinKU. (3) For any check-in p_n^i , if $Pr(p_n^i) > 0$, we connect p_n to the location $p_n^i.s$, and connect the corresponding p'_n to s' . Clearly the mapping can be done in polynomial time. Consequently, EMA is equivalent to deciding, given k and τ , whether MinKU problem can find k subsets S' such that $|\cup_{s'_i \in S'} s'_i| \leq \tau$. If the answer is Yes, then EMA can find $|S'| - k$ locations from \mathcal{S} that saves $|\mathcal{P}| - |\cup_{s_i \in S} S_i|/2 \geq |\mathcal{P}| - \tau/2$ persons. This is because, for a checkpoint, people who connects to it will be healthy as they only have two check-ins. Therefore, for a set of locations that are not checkpoints S , the maximum number of infected persons is $|\cup_{s_i \in S} S_i|/2$. Since MinKU is NP-complete, the decision problem of EMA is NP-complete. Hence, the optimization problem of EMA is NP-hard. \square

C. Algorithm 1. CPT-based Station Selection (CPT-SS)

According to Definition 3, given a set of checkpoints S , we have $W(S)$ that captures the set of people who can be covered (i.e., saved from being infected) if checkpoints are placed at the set S . Accordingly, we define $W(S|s_i) = |W(S \cup \{s_i\})| - |W(S)|$ as the marginal gain of adding s_i into S . A naive greedy-based solution will iteratively select a POI with the maximum $W(S|s_i)$. However, the challenge is how to efficiently evaluate $W(S|s_i)$. Hence, we introduce the CPT-based POI Selection (CPT-SS).

Definition 4. *CPT: Given a person $p_n \in \mathcal{P}$, the Contact Paths Tracing (CPT) of p_n is the set of check-in records in \mathcal{T} that can infect p_n .*

Intuitively, a CPT is generated based on the latest check-in record made by a person $p_n \in \mathcal{P}$ and it includes all the check-in records tr that have a certain probability (> 0) of infecting the person p_n based on the given infectious model. We generate an CPT set as following:

Generation of one CPT.

1. Randomly select $p_n \in \mathcal{P}$; initialize an empty queue Q and an empty CPT;
2. Add tr_i into both Q and CPT where $tr_i \in p_n.Tr$ refers to the latest check-in record made by p_n ;
3. Pop the top record tr_i out of Q ;
4. For each incoming edge of tr_i (from node p_m^j), flip a coin with $Pr(p_n^i, p_m^j)$ probability;
5. If true and $tr_j \notin CPT$, add tr_j into both Q and CPT.
6. Repeat steps 3 to 5 until Q is empty.

According to Definition 4, all records in the CPT of a person p_n can infect p_n . It has been proven that the probability of CPT overlapping with any set of records T is equivalent to the probability of T infecting p_n [49–51]. Thus, the number of times a record tr_i appearing in the CPT set of different persons indicates the potential impact of tr_i in terms of the capability to spread the virus, e.g., the record appearing in the largest number of CPT contributes the most to the spread of the virus and hence shall be isolated first. The last question is how many CPT we need to accurately evaluate $W(S|s_i)$.

Let θ be the number of CPT sets that we need, $\mathcal{F}(S)$ be the fraction of CPT sets over all CPT sets covered by a given set of checkpoints S . The existing work [51] shows that, $n\mathcal{F}(S)$ is an accurate estimator of $W(S)$, when θ is sufficiently large, i.e., $\theta \geq n(8+2\epsilon)(l \log n + \log \binom{n}{k} + \log 2)/(OPT \cdot \epsilon^2)$, where n is the number of check-ins and ϵ is the approximate ratio. OPT can be estimated by $n(1 - (1 - w(CPT))^k)$, where $w(CPT)$ is the number of edges of CPT . For more details of deriving θ , please refer to the work [51].

Algorithm 1 presents the pseudo-code of CPT-SS. To minimize the number of infected persons, we need to find POIs that have the largest coverage, i.e., able to block the most dangerous check-in records that may infect a large number of persons. Since the most dangerous check-in record is expected to appear in the most number of CPT sets, we generate CPT sets and then find checkpoints that can detect the largest

Algorithm 1: CPT-based Station Selection (CPT-SS)

Input: Checkpoint number k , Timeline Graph G , θ
Output: Checkpoint set S

```
1.1 Based on  $G$ , generate  $\theta$  CPT set into  $\mathcal{R}$ 
1.2 while  $|S| \leq k$  do
1.3   Select  $S_i \in \mathcal{S}$  that covers the most CPT sets in  $\mathcal{R}$ 
1.4    $S \leftarrow S \cup \{s_i\}$ 
1.5    $\mathcal{S} \leftarrow \mathcal{S} \setminus \{s_i\}$ 
1.6   Remove all CPT sets covered by  $s_i$  from  $\mathcal{R}$ 
```

number of dangerous check-in records. We first generate θ CPT sets as \mathcal{R} based on the timeline contact graph G (Line 1.1). In the selection loop, we select a POI s_i that covers the most CPT sets in \mathcal{R} (Lines 1.3-1.5), and remove all CPT sets that are covered by s_i from \mathcal{R} (Line 1.6). The loop terminates when $|S| = k$, and S is returned.

VI. EPIDEMIC MAXIMIZED SPREAD IN PUBLIC AREA

In the previous section, we study the EMA problem that aims to find k checkpoints to mitigate the virus diffusion. In this section, from the offensive perspective, we aim to find k ‘super-spreaders’, a small group of persons that will spread the virus the most thus possibly leading to a pandemic. This is necessary and critical to the government to evaluate the robustness of checkpoint deployment strategies in the extreme case that the virus is spread widely.

A. Problem Definition of ESA

We first define the Epidemic Maximized Spread in Public Area (ESA) problem. Our goal is to evaluate the effectiveness of a given checkpoint deployment strategy in the worst case. Specifically, given a checkpoint deployment strategy, we aim to find k persons such that if they are infected at the beginning, they can cause the largest number of persons infected.

With considering the checkpoint, we have the infection probability between two records as below:

$$Pr(p_n^i, p_m^j) = \begin{cases} f(R(\cdot)) & \text{otherwise} \\ 0 & \text{if } tr_i \in S \vee tr_j \in S \end{cases} \quad (2)$$

where S refers to a set of checkpoints. Intuitively, any infected person is unable to infect others at any check point, since he will be placed on quarantine. Based on Equation 2, we introduce the ESA problem formally as follows.

Definition 5. *ESA problem: Given a person dataset \mathcal{P} , a check-in record dataset \mathcal{T} , a set of infected persons $P \in \mathcal{P}$, a set of checkpoints S , a budget k , and an incubation period γ , ESA is to find at most k persons $P \in \mathcal{P}$ such that P can maximize the following equation:*

$$P = \operatorname{argmax}_{|P| \leq k} I_{\mathcal{P}, \mathcal{T}, \gamma, S}(P). \quad (3)$$

Algorithm 2: CPT-based Person Selection

Input: Person number k , Timeline Graph G , A
checkpoint set S

Output: Person set P

```
2.1 Based on  $G$ , generate  $\theta$  CPT set into  $\mathcal{R}$  according to
    the updated Step 4
2.2 while  $|P| \leq k$  do
2.3   Select  $p_i \in \mathcal{P}$  that covers the most CPT sets in  $\mathcal{R}$ 
2.4    $P \leftarrow P \cup \{p_i\}$ 
2.5    $\mathcal{P} \leftarrow \mathcal{P} \setminus \{p_i\}$ 
2.6   Remove all CPT sets covered by  $p_i$  from  $\mathcal{R}$ 
```

B. Hardness of ESA

Theorem 2. *The ESA problem is NP-hard.*

Proof. We prove it by reducing the Set Cover problem to the ESA problem. In the Set Cover problem, given a collection of sets $S' = \{s'_1, s'_2, \dots, s'_m\}$ where each set s'_i is a subset of a given ground set $\mathcal{P}' = \{p'_1, \dots, p'_n\}$, it aims to find whether there exist k of the subsets whose union is equal to \mathcal{P}' . We reduce the Set Cover problem to ESA with the following process: (1) We map each element $p'_i \in \mathcal{P}'$ in the Set Cover problem to each person $p_i \in \mathcal{P}$ in the ESA problem. (2) We map each set $s'_i \in S'$ in the Set Cover Problem to a set of persons $\{p_i, \dots, p_j\} = I(p_n) \subseteq \mathcal{P}$ in the ESA problem, where $p'_m \in s'_n$ maps to the person $p_m \in I(p_n)$ that will be infected by p_n . Consequently, the Set Cover problem is equivalent to deciding whether there are the k -sized set of initially infected persons $P \in \mathcal{P}$, such that $I(P) = |\mathcal{P}|$. Because the Set Cover problem is NP-complete, the decision problem of EMA is NP-complete. Hence, the optimization problem of EMA is NP-hard. \square

C. Algorithm 2. CPT-based Person Selection (CPT-PS)

Now, we are ready to present the solution, CPT-based Person Selection (CPT-PS), for the ESA problem. The main objective is to find the set of super-spreaders, with each being able to infect many healthy persons. Similar to the EMA problem, a super-spreader is a person whose records appear in the most number of CPT sets. Based on the timeline contact graph G , we initialize and generate θ number of CPT sets as \mathcal{R} first. Then, a person p_i that covers the largest fraction of CPT sets is added into P ; and all CPT sets that are covered by p_i are removed from \mathcal{R} . The loop terminates when $|P| = k$, and P is returned. It is worth noting that there is one difference between ESA and EMA, the process of generating a CPT. According to Definition 2, if an infected person p_n checks-in at s via tr_i , p_n will be isolated and $p_n.Tr = \{tr_i, \dots, tr_{|Tr|}\}$ will be removed from \mathcal{T} . Moreover, the CPT of p_n is the set of check-in records in \mathcal{T} that can infect $p_n^{|Tr|}$. Therefore, an infected trip is not able to infect p_n for the CPT of p_n . As a result, in the process of generating CPT, we change Step 4 to: for each incoming edge of tr_i , if $tr_i.s \notin S$, flip a coin with $Pr(p_n^i, p_m^j)$ probability, where S is the set of checkpoints.

VII. EXPERIMENT

In this section, we evaluate the effectiveness and the efficiency of our solutions. First, we introduce two infection probability measurements that are common in the epidemic field in Section VII-A. Recall that our work is independent of the choice of infection probability $f()$ and hence we take $f()$ as an input to our framework. Second, we introduce the datasets in Section VII-B and present the detailed experiment setup in Section VII-C. Last but not least, we report the experimental results from Section VII-D to Section VII-F.

Evaluation Purposes. As stated in Section I, we would like to achieve two goals: 1) Tracing Close Contacts in Short-term, and 2) Deploying Checkpoints in Short-term. Accordingly, we conduct two different sets of experiments. First, we evaluate how accurately and efficiently our timeline contact graph models the virus diffusion as compared to the dynamic graph with different snapshots, and present the results in Section VII-D. Second, we evaluate how well the various algorithms could mitigate the epidemic from a set of infected persons from two perspectives. (1) *Defensive perspective*: a set of infected persons that are randomly chosen (the EMA problem) in Section VII-E; (2) *Offensive perspective*: a set of infected persons who are specifically selected to maximally attack checkpoints (the ESA problem) in Section VII-F.

A. Infection Probability Measurement

As described in Section III-B, $f()$ denotes the infection probability and $R()$ is the exposure duration. To demonstrate that our work can take any infection probability $f()$ as an input, we adopt two different models with unique $f()$ for illustration. The first model follows studies in the virus domain [17, 18, 35] and sets $f(R) = 1/(1 + (EC_{50}/R)^\tau)$, where EC_{50} is a time threshold that a healthy person will have a 50% probability of being infected if she stays in the same POI closely with another infected person; τ is used to adjust the slope of $f()$. We name it as EC_{50} , and set $\tau = 3$. The second model is based on a threshold of exposure duration, which we name as $InfTre$. Specifically, given a threshold of exposure duration, $f() = 100\%$ if $R()$ is not shorter than the threshold, and $f() = 0\%$ otherwise. For example, for the COVID-19, more than 15 minutes of contact can be considered as highly infectious [3]. Therefore, we set the threshold of $InfTre$ to 15 minutes. We have $f() = 100\%$ if $R() \geq 15$ minutes, and $f() = 0\%$ otherwise.

We adopt the EC_{50} model as the default model and present the experimental results of $InfTre$ model in Section VII-G. It is worth noting that, the overall observations that we make from two models are consistent. Again, we want to highlight that the choice of measurement $f()$ is orthogonal to this work so long as $f()$ is related to the exposure duration.

B. Datasets

As reported in Table III, we use two different EZ-LINK datasets recording trips of different months (provided by the authors of [52]). We adopt the first dataset in our experimental study as the default dataset. The second dataset is used to

TABLE III: Statistics of Datasets

| Dataset | $ \mathcal{T} $ | $ \mathcal{P} $ | $ \mathcal{S} $ | Period |
|---------|-------------------|-------------------|-----------------|---------|
| D-1 | 2×10^6 | 5.2×10^4 | 4962 | 14 days |
| D-2 | 1.3×10^7 | 6.3×10^5 | 4962 | 28 days |

TABLE IV: Parameter Settings

| | |
|---------------------|--|
| k | 25, 50 , 75 |
| γ (Hours) | 24, 72 , 120 |
| EC_{50} (Seconds) | 1800, 3600 , 7200 |
| Period (Days) | 7, 14 , 21, 28 |
| P_s | 0.01%, 0.05%, 0.1% , 0.2%, 0.5%, 1% |

evaluate the scalability of our solutions with the results to be reported in Section VII-H. EZ-link is a smart card system used in Singapore for public transport. The number of passengers after excluding those taking less than two trips daily is listed in the table. We want to highlight that the scale of the datasets is close to $|\mathcal{P}|/|\mathcal{T}|$ at a city-level.

A trip record from the public transport data is not exactly the same as the check-in record defined in Section III. Our model can be applied to both trip records and check-in records with a slight modification. We define a trip tr_i as a tuple $\{b, s_b, s_e, t_b, t_e\}$. b denotes the riding bus, s_b and s_e denote the boarding station and alighting station respectively, and t_b and t_e are the boarding time and alighting time respectively. The deviation from the original check-in records does not affect the virus diffusion, but only the exposure duration calculation R and the checkpoint. To be more specific, for R w.r.t. trip records, the critical condition is modified as $tr_i.b = tr_j.b$. For normal check-in records, each record is for one POI and there is no s_b or s_e ; for trip records, b refers to the physical bus and s_b and s_e refer to two different stations. Accordingly, we rewrite the definition of a checkpoint as below.

Given a checkpoint s , when an infected person p_n boards or alights at s via trip tr_i , p_n will be isolated before boarding or after alighting at s , i.e., $p_n.Tr = \{tr_i, \dots, tr_{|Tr|}\}$ will be removed from \mathcal{T} .

It is worth noting that, if the infected passenger is identified before boarding, she will be isolated immediately. However, if she is only checked after alighting, although she will be isolated immediately, passengers taking the same bus as her on this trip still run the risk of being infected.

C. Experiment Setup

All key parameters are summarized in Table IV, including the number of checkpoints k , the incubation period γ , and the threshold of contact time EC_{50} . In each set of experiments, we vary only one parameter and set the rest parameters to their default values highlighted in bold.

Incubation period γ . This is a period between when a passenger is able to infect others and when she is infected. It varies from disease to disease. For instance, the average incubation of Influenza is two days [53], and that of COVID-19 is five days [2, 54]. Hence, we set γ to 24 hours (1 day), 72 hours (3 days), and 120 hours (5 days), to represent short, normal, and long incubation periods to cover most cases.

Transmissibility EC_{50} . As aforementioned in Section VII-A, a smaller EC_{50} indicates that the healthy passengers are more easily infected. The longer the contact time they have, the higher the infected probability is, and vice versa. In our study, we set EC_{50} to 1,800 seconds, 3,600 seconds, and 5,400 seconds, which represent high, normal, and low transmissibility.

Percentage of Initially Infected Passengers P_s . The number of initially infected passengers is important. The earlier the government is involved in the epidemic, the fewer the initially infected passengers. Accordingly, it will be easier to mitigate the epidemic. A straightforward setup is to assume different numbers of initially infected passengers, e.g., 1,000 or 10,000. However, a fixed number is meaningless without considering the total number of passengers. Therefore, we set P_s as the percentage of the passengers that are initially infected. Then, the number of initially infected passengers will be $P_s \times |\mathcal{P}|$, where $|\mathcal{P}|$ is the total number of passengers. In each experiment, we set P_s to 0.01%, 0.05%, 0.1%, 0.2%, 0.5%, and 1%, which represent the cases from a few initially infected persons to a small group of initially infected persons.

Experiment Environment. All codes are implemented in Java. They are available online¹ for reproducibility. All experiments are conducted on a machine with a CPU of Intel Core i7-8750U, 32GB RAM and running Windows 10 OS.

Performance Metrics. The total number of infected passengers and the running time are employed as the effectiveness metric and the efficiency metric respectively. For each experiment, we report the average result of 20 runs.

Compared Methods. The comparison is conducted from two perspectives, w.r.t. two different goals presented earlier.

- 1) **Diffusion Models:** we compare our TCG with the dynamic graph [16] of different durations, i.e., Dy- x . Here, Dy- x stands for dynamic graph with snapshots and x refers to the number of hours between two consecutive snapshots (i.e., a smaller x value indicates that more snapshots will be generated based on a shorter interval). Each snapshot is a graph $G = (V, E)$ representing the contact information of all passengers, where V is the set of passengers. For every two passengers v_i and v_j , there will be an edge connecting them if within the duration of x -hours they have a contact (i.e., have check-in records in the same location). The weight of the edge is the infection probability, that is measured as $f(R)$, where R is the shortest time that v_i or v_j stays at the location.
- 2) **Checkpoints Deployment Strategies:** (1) For the EMA problem, we compare three deployment strategies: i) Top- k : k checkpoints that cover the largest number of trips, ii) CPT-SS: the CPT-based checkpoints selection (Section V-C), and iii) Eig: the eigenvalue-based solution presented in Section II-A. Despite the different goals, most of VI studies are based on an eigenvalue solution [7–11, 24–28]. Therefore, we build the Eig baseline using the same methodology. The weight of an edge between

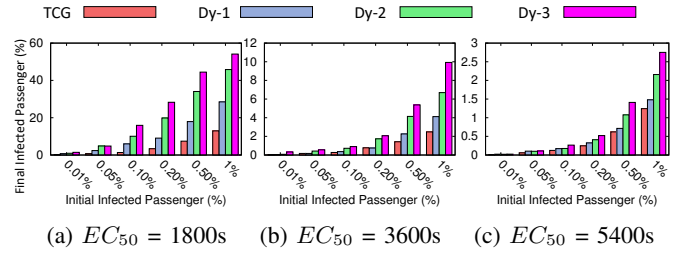


Fig. 3: Graph Competition of varying EC_{50} (Seconds) when incubation $\gamma = 72$ hours within 7 days

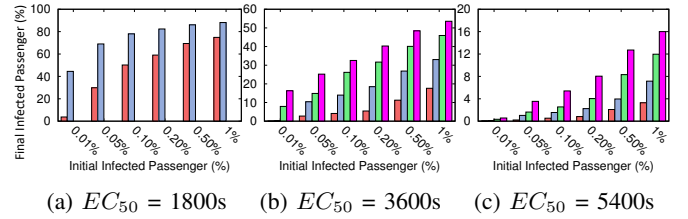


Fig. 4: Graph Competition of varying EC_{50} (Seconds) when incubation $\gamma = 72$ hours within 14 days

nodes is the normalized value that refers to the number of trips connecting them. In each iteration, we select a node that maximizes the decrease of the first eigenvalue. (2) For the ESA problem, we compare two different sets of initially infected passengers: i) *Rand*: P_s randomly-selected passengers, and ii) *Max*: P_s super-spreaders identified by CPT-PS (Section VI-C).

D. Evaluation of The Timeline Contact Graph

In our first set of experiments, we compare the accuracy and efficiency of our TCG and the dynamic graph in terms of modelling the virus diffusion without checkpoints. We vary two parameters, the transmissibility EC_{50} and the incubation period γ . As mentioned in Section III-B, the lower the EC_{50} and γ are, the faster the breakout of a disease is. Therefore, a small EC_{50} and a small γ require accurate modelling. All initially infected passengers are randomly picked. Figures 3 - 6 show the experimental results. We make the following four main observations.

First, TCG can more accurately model the finally infected passengers. For instance, in Figure 3b, when $P_s = 0.1\%$, Dy-1, Dy-2 and Dy-3 overestimate the number of infections by 1.6 times, 2.9 times and 3.8 times than TCG, respectively. This is because when the model is based on the snapshots, the temporal orders of trip records might not be accurately captured, e.g., two passengers will be regarded as close contacts when they appear in the same bus within one snapshot, even though the durations they stay in the bus do not overlap. Example 2 illustrates how the snapshot-based solution inaccurately models the virus spreading. In order to correctly capture the contacts between all passengers, it requests a new snapshot whenever there is an arriving/leaving passenger. Obviously, it is impractical to track virus diffusion using dynamic graphs for a public system that has millions of passengers.

¹<https://github.com/rmitbgroup/VirusPrediction>

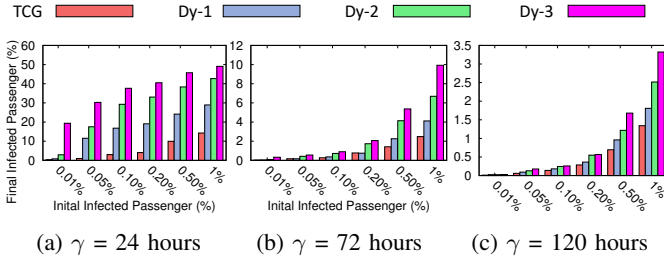


Fig. 5: Graph Competition of varying γ when incubation $EC_{50} = 3600$ seconds within 7 days

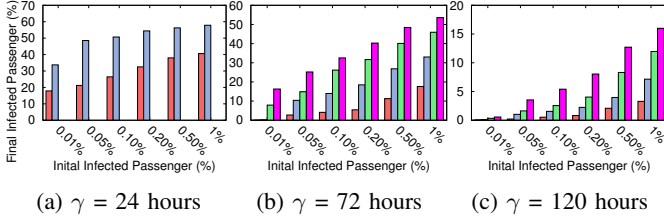


Fig. 6: Graph Competition of varying γ when incubation $EC_{50} = 3600$ seconds within 14 days

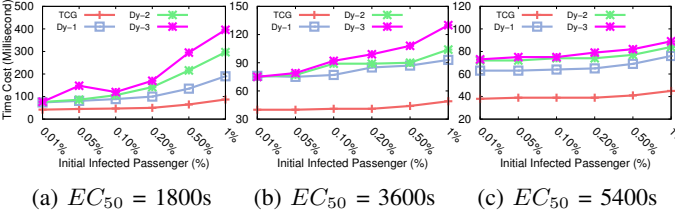


Fig. 7: Running Time of varying EC_{50} (Second) when incubation $\gamma = 72$ hours within 7 days

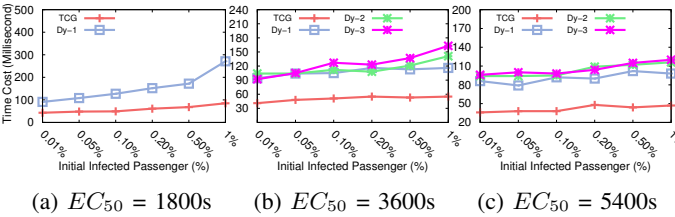


Fig. 8: Running Time of varying EC_{50} (Second) when incubation $\gamma = 72$ hours within 14 days

Second, the advantage of TCG becomes more significant when EC_{50} becomes smaller. For example, when $EC_{50} = 1,800$ s, in terms of the number of infected persons, TCG outperforms Dy-1, Dy-2, and Dy-3 by 4.4 times, 7.5 times, and 11.9 times respectively, as shown in Figure 3a.

Third, with an increasing prediction period (i.e., from 7 days to 14 days), the overestimation of dynamic graph of different durations becomes even larger and the concern on efficiency becomes more severe. In Figure 4a, Dy-2 and Dy-3 are unable to finish the modelling due to memory overflow. Even Dy-1 that takes one snapshot per hour is not able to achieve a good accuracy and an even higher frequency is required to enhance the accuracy as the number of overestimation (even under Dy-1) is huge.

Last, the experimental results reported in Figure 5 and Figure 6 demonstrate a similar trend. When EC_{50} is small, a

short exposure duration may lead to an infection. This in turn will cause an explosive increase in the number of infected passengers, since dynamic graph (based on snapshots) mistakenly considers non-contact passengers as having contact. Therefore, given a small EC_{50} , it is very easy for dynamic graph to overestimate the number of infected passengers. For the same reason in Figure 4a, we omit the results of Dy-2 and Dy-3 in Figure 6a.

We also evaluate the efficiency of different methods and the results are reported in Figure 7 and Figure 8. It is worth noting that we only report the running time of modelling the virus diffusion but exclude the time required to build checkpoints. We have the following observations.

Consistent with our expectation, TCG requires significantly less time, as compared with dynamic graph. For dynamic graphs, a short interval between snapshots will obviously accelerate the modelling. Apparently, compared with the 7-day prediction, the 14-day prediction has a higher running time for all models. One interesting point is that, with a larger EC_{50} , the increase of P_s shows a smaller impact on the running time. It is because a large EC_{50} can avoid the explosive growth of the final infection number. Therefore, the larger the EC_{50} is, the smaller the impact of P_s on running time is. In Figure 8c, results of Dy-2 and Dy-3 are not reported. This is because they both are out of memory as they generate a massive number of edges due to the inaccurate contact recording.

E. Evaluation of Checkpoints Deployment Strategies to Address the EMA Problem

1) Effectiveness Study:

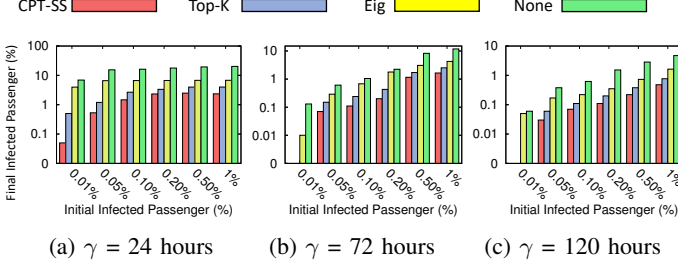
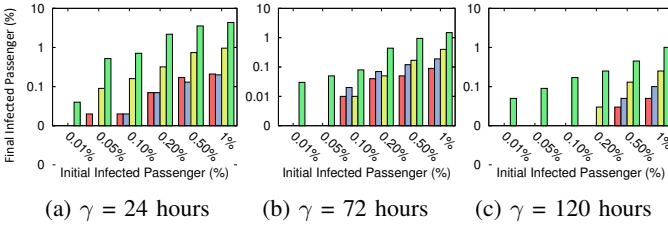
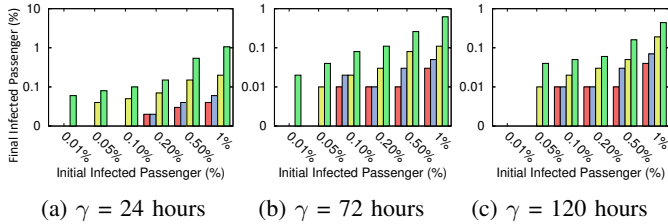
In this part, we evaluate different algorithms in terms of how well they can mitigate the virus diffusion under different settings of γ and EC_{50} . As aforementioned in Section III, the incubation period γ and transmissibility EC_{50} determine how easily a virus could be spread. Specifically, under the default number of checkpoints ($k = 50$), we simulate three different categories corresponding to the virus of low/medium/high danger, which lead to nine scenarios, as summarized in Table V, together with the corresponding results.

For each scenario, we vary the percentage of initially infected passengers, P_s , from 0.01% to 1%, to simulate how serious the epidemic is. Here, we adopt the *Rand* setting, i.e., $P_s \times |\mathcal{P}|$ randomly selected passengers are considered to be initially infected. For evaluating how the algorithms CPT-SS, Top- k , and Eig mitigate the virus diffusion compared to the case without deploying checkpoints, the experimental results of none-checkpoint have been presented with a green bar and named as “None”. Figures 9-11 show the experimental results where we make five main observations.

First, with a larger P_s , all the algorithms result in a larger number of finally infected passengers. It is clear that an early adoption of the measures to control the virus spread could help mitigate the epidemic. Moreover, when both γ and EC_{50} are small, the virus is highly contagious, and hence a few infected passengers will lead to a huge number of infected passengers.

TABLE V: Effectiveness Experiment Setup

| γ | | EC_{50} | | |
|-------------------------------|-------|--------------------------------|------------|------------|
| | | High \longleftrightarrow Low | | |
| High \updownarrow Low | 1800s | 24h | 72h | 120h |
| | 3600s | Figure 9a | Figure 9b | Figure 9c |
| | 5400s | Figure 10a | Figure 10b | Figure 10c |

Fig. 9: Infection of varying incubation γ when $EC_{50}=1800s$ Fig. 10: Infection of varying incubation γ when $EC_{50}=3600s$ Fig. 11: Infection of varying incubation γ when $EC_{50}=5400s$

Second, with a fixed EC_{50} , the smaller the incubation period γ is, the bigger the number of finally infected passengers will be. This is because when γ is small, a passenger will soon be able to infect others after she is infected.

Third, with a fixed γ , when EC_{50} becomes larger, the numbers of finally infected passengers under all the algorithms become smaller. This is because a larger EC_{50} indicates that healthy passengers will be less likely infected.

Fourth, CPT-SS outperforms Top- k and Eig by three times and ten times, respectively. The poor performance of Top- k reflects that establishing checkpoints based on passenger flow is less effective. On the other hand, Eig is unable to find right locations to build checkpoints due to the inaccurate contact recording. It is worth noting that eigenvalue-based solutions severely suffer from the scalability issue. For example, in order to calculate the eigenvalue for a dataset with 1.3×10^7 trips, it requests an adjacent matrix of size $(1.3 \times 10^7)^2$. Neither the storing of this matrix nor the calculation of the eigenvalue of this matrix is practical.

Fifth, the advantage of CPT-SS becomes more significant

TABLE VI: Efficiency Study of CPT-SS (Second)

| Period | | γ | k | EC_{50} | | |
|--------|-----|----------|--------|-----------|--------|------|
| | | | | 1800 | 3600 | 5400 |
| 7 | 24 | 25 | 31.02 | 62.68 | 88.92 | |
| | | 50 | 27.88 | 50.14 | 67.72 | |
| | | 75 | 32.06 | 55.35 | 61.22 | |
| | 72 | 25 | 42.98 | 65.34 | 72.12 | |
| | | 50 | 30.12 | 48.89 | 56.3 | |
| | | 75 | 33.35 | 45.17 | 50.72 | |
| | 120 | 25 | 52.31 | 62.51 | 80.59 | |
| | | 50 | 37.06 | 45.12 | 55.1 | |
| | | 75 | 36.36 | 44.77 | 61.95 | |
| 14 | 24 | 25 | 75.68 | 137.01 | 201.4 | |
| | | 50 | 85.93 | 143.08 | 161.55 | |
| | | 75 | 145.45 | 178.85 | 162.15 | |
| | 72 | 25 | 72.17 | 179.73 | 191.5 | |
| | | 50 | 61.26 | 133.8 | 143.84 | |
| | | 75 | 66.49 | 127.85 | 139.36 | |
| | 120 | 25 | 102.57 | 164.63 | 183.4 | |
| | | 50 | 77.87 | 128.38 | 140.44 | |
| | | 75 | 73 | 123.17 | 141.42 | |

when the epidemic situation is more serious (i.e., $\gamma = 24$ hours or $EC_{50} = 1,800$ seconds or $P_s \geq 1\%$). This is because when the virus is highly contagious, it is easy to cause an epidemic without planning the deployment of checkpoints carefully. On the other hand, when the virus is relatively less harmful, both algorithms are able to mitigate the epidemic.

In addition, we test how the number of finally infected passengers changes by varying the number of checkpoints k (i.e., 25, 50, and 75), and report the results in Figure 12. We make the following three observations.

First, with more checkpoints, the number of finally infected passengers becomes smaller. Second, with more checkpoints ($k = 75$), the average advantage of CPT-SS becomes more significant. This is because checkpoints are only able to control the spread of virus to certain degree. When k is large, since the high volume stations may only located at city, the coverage of them are overlapped, and hence other locations may be missed. Third, when the group of initially infected passengers is bigger (i.e., $P_s \geq 0.5\%$), the advantage of CPT-SS becomes more significant. The reason is the same as the second one. When there are more initially infected passengers, the pandemic situation becomes more serious. If the deployment strategy could not allocate the limited checkpoints well but “waste” resources (i.e., overlapped coverage), some locations may be missed, and hence causes more infected passengers.

2) Efficiency Study:

The condition of the epidemic changes quickly. The government may need to review and adjust the deployment strategy frequently (e.g., in a daily basis) based on updated epidemic situation. Hence, the efficiency of our mitigation algorithm CPT-SS is critical. We have three main observations.

First, the increasing EC_{50} will increase time-cost. According to existing studies [49–51], a smaller infection probability leads to a smaller average width of CPT (contact paths tracing), which in turn requests a larger number of CPT to evaluate each trip’s infection range, hence more time are

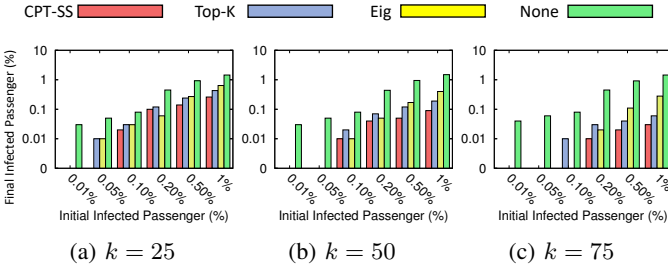


Fig. 12: Infection of varying the checkpoint number k

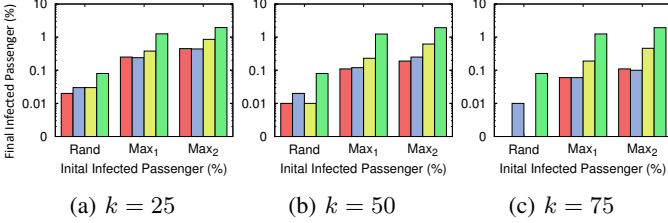


Fig. 13: Robustness Evaluation

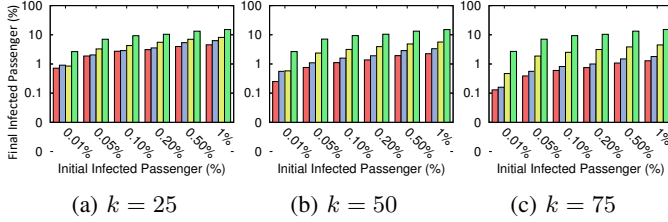


Fig. 14: Evaluation of influence models when the threshold of exposure duration is 15 minutes.

needed. Second, the number of checkpoints only slightly affects the time-cost of CPT-SS. Intuitively, this is because, when the number of checkpoints increases, we do not need a highly accurate evaluation of the coverage of checkpoints since a larger number will “remedy” the accurate losing. Third, the varying period will hugely affect the time-cost. The reason is that the extending period will contain more trips, increasing the size of the graph, and hence we need more CPT.

F. Evaluation of the Impact of Super-spreader in ESA

As described in Goal 2 in Section I, from the offensive perspective, we first find a set of ‘super-spreaders’ who are a small group of persons that will spread the virus the most, thus possibly leading to a pandemic; we then set this set of ‘super-spreaders’ as the initially infected passengers and evaluate the robustness of checkpoint deployment strategies.

In order to demonstrate the potential impact of ‘super-spreaders’, we have to generate ‘super-spreaders’ P . In our study, we adopt two strategies, Max_1 and Max_2 based on the CPT-PS (i.e., Algorithm 2). The difference is that, in Max_1 , CPT-PS generates P without knowing the checkpoints S . In other words, there are few infected passengers riding the public transportation which have the highest passenger flow. Therefore, it tries to simulate a general worst case. In contrast, in Max_2 , CPT-PS generates P with the knowledge of the detailed deployment of checkpoints S . Therefore, P

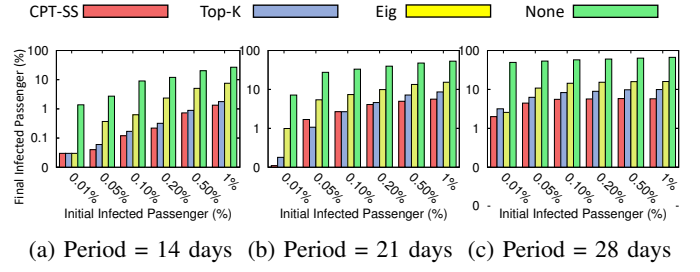


Fig. 15: Scalability - Varying period

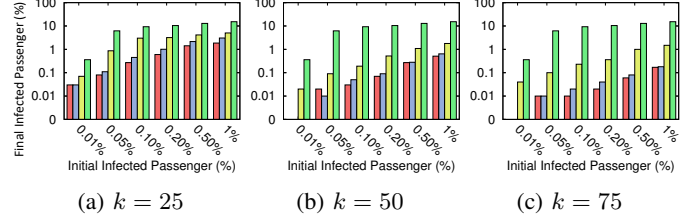


Fig. 16: Scalability - Varying k when $EC_{50} = 3600s$ and $\gamma = 72$ hours

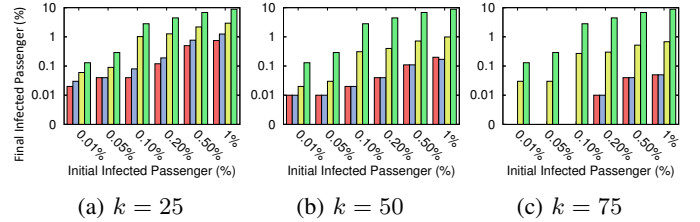


Fig. 17: Scalability - Varying k when $EC_{50} = 3600s$ and $\gamma = 120$ hours

is specifically generated to attack S . In addition, we also implement *Rand*, which assumes that all initially infected passengers are selected from \mathcal{P} with an equal probability. The experimental results are plotted in Figure 13, and we have three observations.

First, among all experimental results, the number of finally infected passengers of *Rand* is smaller than that of Max_1 and Max_2 . It proves that ‘super-spreaders’ do have a higher risk of causing the pandemic.

Second, the larger the number of checkpoints is, the more significant the advantage of CPT-SS is. When there are not enough checkpoints, we cannot protect the entire population even when we are able to locate the ‘super-spreaders’. As the number of checkpoints increases, it becomes easier and more effective for CPT-SS to deploy checkpoints to block the ‘super-spreaders’. It also demonstrates that establishing checkpoints based purely on passenger flow is less effective.

Third, all solutions have a worse result in Max_2 . It is because, in Max_2 , the initially infected passengers are selected specifically to attack checkpoints. Even though, our solution CPT-SS still outperforms others.

G. Evaluation of Influence Models (EC_{50} v.s. $InfTre$)

Though EC_{50} is the default model, we also evaluate the other influence model, i.e. the *InfTre* model. As aforementioned,

TABLE VII: Scalability Study of CPT-SS when Period is 28 days (Second)

| | | | | Random | | | | | | Max | | | | | | |
|----------|--------|-----------|--------|--------|--------|--------|--------|--------|--------|--------|--------|--------|--------|--------|--------|--------|
| γ | k | EC_{50} | P | 0.01% | 0.05% | 0.10% | 0.20% | 0.50% | 1% | 0.01% | 0.05% | 0.10% | 0.20% | 0.50% | 1% | |
| 72 | 25 | 3600 | CPT-SS | 0.10% | 7.02% | 8.72% | 10.13% | 10.52% | 10.68% | 7.45% | 9.66% | 10.16% | 10.42% | 10.43% | 10.74% | |
| | | | TOP-K | 0.12% | 10.08% | 12.09% | 13.85% | 14.58% | 14.86% | 10.17% | 13.24% | 14.08% | 14.49% | 14.68% | 15.07% | |
| | | | Eig | 0.65% | 15.27% | 16.77% | 18.15% | 18.68% | 18.84% | 14.96% | 18.20% | 18.42% | 18.57% | 18.54% | 18.52% | |
| | | | None | 13.71% | 36.99% | 42.16% | 44.52% | 46.74% | 47.84% | 37.89% | 44.86% | 45.99% | 46.93% | 48.08% | 48.85% | |
| | | 5400 | CPT-SS | 0.03% | 0.08% | 0.27% | 0.60% | 1.42% | 1.86% | 0.88% | 1.23% | 1.66% | 1.93% | 2.36% | 2.77% | |
| | | | TOP-K | 0.03% | 0.11% | 0.45% | 1.01% | 2.16% | 3.06% | 1.33% | 1.88% | 2.46% | 2.88% | 3.55% | 4.09% | |
| | | | Eig | 0.07% | 0.87% | 3.02% | 3.18% | 4.15% | 5.04% | 2.85% | 3.96% | 4.68% | 5.07% | 5.68% | 6.16% | |
| | | | None | 0.36% | 6.20% | 9.33% | 10.45% | 12.90% | 15.24% | 7.95% | 10.63% | 13.29% | 14.41% | 16.16% | 17.48% | |
| | | 3600 | CPT-SS | 0.02% | 1.75% | 3.20% | 4.06% | 4.25% | 4.44% | 0.31% | 3.57% | 4.04% | 4.18% | 4.28% | 4.36% | |
| | | | TOP-K | 0.01% | 2.00% | 3.75% | 4.80% | 5.04% | 4.65% | 2.46% | 4.13% | 4.81% | 4.97% | 5.12% | 5.38% | |
| | | | Eig | 3.48% | 6.01% | 7.59% | 8.21% | 8.47% | 8.65% | 1.05% | 8.06% | 8.15% | 8.25% | 8.46% | 8.65% | |
| | | | None | 16.42% | 27.80% | 31.18% | 32.47% | 33.30% | 33.77% | 28.42% | 32.10% | 32.85% | 33.26% | 33.64% | 33.88% | |
| | 50 | 3600 | CPT-SS | 0.00% | 0.02% | 0.03% | 0.07% | 0.27% | 0.51% | 0.04% | 0.26% | 0.44% | 0.48% | 0.59% | 0.77% | |
| | | | TOP-K | 0.00% | 0.01% | 0.05% | 0.09% | 0.28% | 0.64% | 0.09% | 0.17% | 0.46% | 0.57% | 0.82% | 1.03% | |
| | | | Eig | 0.02% | 0.09% | 0.19% | 0.52% | 1.09% | 1.78% | 0.22% | 1.26% | 1.65% | 1.82% | 2.10% | 2.37% | |
| | | | None | 0.36% | 6.20% | 9.33% | 10.45% | 12.90% | 15.24% | 7.95% | 10.63% | 13.29% | 14.41% | 16.16% | 17.48% | |
| | | 5400 | CPT-SS | 0.00% | 0.01% | 0.02% | 0.04% | 0.08% | 0.18% | 0.02% | 0.06% | 0.16% | 0.18% | 0.26% | 0.33% | |
| | | | TOP-K | 0.00% | 0.01% | 0.02% | 0.04% | 0.08% | 0.18% | 0.02% | 0.06% | 0.16% | 0.18% | 0.26% | 0.33% | |
| | | | Eig | 0.04% | 0.10% | 0.23% | 0.36% | 1.00% | 1.49% | 0.02% | 1.02% | 1.46% | 1.64% | 1.95% | 2.19% | |
| | | | None | 0.36% | 6.20% | 9.33% | 10.45% | 12.90% | 15.24% | 7.95% | 10.63% | 13.29% | 14.41% | 16.16% | 17.48% | |
| | | 75 | 3600 | CPT-SS | 0.00% | 0.78% | 1.45% | 1.89% | 2.18% | 2.25% | 0.00% | 1.64% | 1.92% | 2.12% | 2.18% | 2.28% |
| | | | | TOP-K | 0.00% | 1.01% | 1.67% | 2.37% | 2.59% | 2.64% | 0.88% | 1.96% | 2.26% | 2.47% | 2.55% | 2.94% |
| | | | | Eig | 2.49% | 4.89% | 6.31% | 6.82% | 6.80% | 6.74% | 0.93% | 6.73% | 6.72% | 6.61% | 6.40% | 6.17% |
| | | | | None | 13.71% | 36.99% | 42.16% | 44.52% | 46.74% | 47.84% | 37.89% | 44.86% | 45.99% | 46.93% | 48.08% | 48.85% |
| 5400 | CPT-SS | | 0.00% | 0.01% | 0.01% | 0.02% | 0.06% | 0.17% | 0.00% | 0.06% | 0.10% | 0.13% | 0.18% | 0.26% | | |
| | TOP-K | | 0.00% | 0.01% | 0.02% | 0.04% | 0.08% | 0.18% | 0.02% | 0.06% | 0.16% | 0.18% | 0.26% | 0.33% | | |
| | Eig | | 0.04% | 0.10% | 0.23% | 0.36% | 1.00% | 1.49% | 0.02% | 1.02% | 1.46% | 1.64% | 1.95% | 2.19% | | |
| | None | | 0.36% | 6.20% | 9.33% | 10.45% | 12.90% | 15.24% | 7.95% | 10.63% | 13.29% | 14.41% | 16.16% | 17.48% | | |
| 120 | 25 | | 3600 | CPT-SS | 0.04% | 0.60% | 2.12% | 2.92% | 4.83% | 6.41% | 2.22% | 2.91% | 4.43% | 5.93% | 7.70% | 8.50% |
| | | | | TOP-K | 0.07% | 0.99% | 2.82% | 4.53% | 7.31% | 9.14% | 2.93% | 4.42% | 6.20% | 8.51% | 10.75% | 11.74% |
| | | | | Eig | 1.05% | 4.27% | 8.07% | 9.65% | 12.39% | 13.67% | 6.24% | 8.25% | 10.86% | 12.95% | 14.74% | 15.74% |
| | | | | None | 5.34% | 18.05% | 23.81% | 26.53% | 32.76% | 35.73% | 17.13% | 25.02% | 29.01% | 33.46% | 37.53% | 39.74% |
| | | 5400 | CPT-SS | 0.02% | 0.04% | 0.04% | 0.12% | 0.50% | 0.75% | 0.05% | 0.27% | 0.51% | 0.92% | 1.51% | 1.97% | |
| | | | TOP-K | 0.03% | 0.04% | 0.08% | 0.19% | 0.77% | 1.25% | 0.07% | 0.43% | 0.79% | 1.34% | 2.31% | 3.02% | |
| | | | Eig | 0.06% | 0.09% | 1.02% | 1.27% | 2.18% | 2.94% | 1.03% | 2.00% | 2.68% | 3.16% | 4.13% | 4.95% | |
| | | | None | 0.13% | 0.29% | 2.81% | 4.46% | 6.83% | 8.88% | 3.31% | 6.39% | 7.90% | 9.62% | 11.99% | 13.83% | |
| | | 3600 | CPT-SS | 0.01% | 0.18% | 0.34% | 0.75% | 1.34% | 2.04% | 0.67% | 0.86% | 1.18% | 1.78% | 2.73% | 3.25% | |
| | | | TOP-K | 0.00% | 0.19% | 0.41% | 1.08% | 1.66% | 2.52% | 0.56% | 0.73% | 1.12% | 2.29% | 3.35% | 3.98% | |
| | | | Eig | 0.37% | 1.69% | 2.88% | 3.68% | 4.71% | 5.52% | 2.42% | 3.30% | 3.94% | 4.94% | 6.20% | 6.70% | |
| | | | None | 4.04% | 13.50% | 17.47% | 20.04% | 24.30% | 26.80% | 13.03% | 18.70% | 21.22% | 24.78% | 28.26% | 29.81% | |
| | 50 | 3600 | CPT-SS | 0.01% | 0.01% | 0.02% | 0.04% | 0.11% | 0.20% | 0.02% | 0.04% | 0.10% | 0.22% | 0.40% | 0.60% | |
| | | | TOP-K | 0.01% | 0.01% | 0.02% | 0.04% | 0.11% | 0.17% | 0.00% | 0.06% | 0.11% | 0.25% | 0.50% | 0.70% | |
| | | | Eig | 0.02% | 0.03% | 0.31% | 0.40% | 0.72% | 0.99% | 0.31% | 0.78% | 0.97% | 1.19% | 1.58% | 1.95% | |
| | | | None | 0.13% | 0.29% | 2.81% | 4.46% | 6.83% | 8.88% | 3.31% | 6.39% | 7.90% | 9.62% | 11.99% | 13.83% | |
| | | 5400 | SIM | 0.00% | 0.03% | 0.07% | 0.21% | 0.49% | 0.82% | 0.27% | 0.39% | 0.51% | 0.74% | 1.27% | 1.52% | |
| | | | TOP-K | 0.00% | 0.04% | 0.09% | 0.30% | 0.58% | 1.02% | 0.36% | 0.45% | 0.61% | 0.89% | 1.53% | 1.87% | |
| | | | Eig | 0.30% | 1.21% | 2.41% | 3.17% | 4.17% | 5.01% | 2.60% | 3.35% | 3.79% | 4.57% | 5.60% | 6.01% | |
| | | | None | 3.87% | 13.88% | 19.01% | 21.47% | 26.76% | 29.35% | 16.24% | 21.78% | 24.19% | 28.00% | 31.17% | 32.75% | |
| | | 75 | 3600 | SIM | 0.00% | 0.00% | 0.00% | 0.01% | 0.04% | 0.05% | 0.00% | 0.01% | 0.03% | 0.08% | 0.12% | 0.19% |
| | | | | TOP-K | 0.00% | 0.00% | 0.00% | 0.01% | 0.04% | 0.05% | 0.00% | 0.01% | 0.03% | 0.09% | 0.15% | 0.22% |
| | | | | Eig | 0.03% | 0.03% | 0.27% | 0.30% | 0.52% | 0.68% | 0.25% | 0.59% | 0.73% | 0.98% | 1.27% | 1.56% |
| | | | | None | 0.13% | 0.29% | 2.81% | 4.46% | 6.83% | 8.88% | 3.31% | 6.39% | 7.90% | 9.62% | 11.99% | 13.83% |

tioned in Section VII-A, the *InfTre* model evaluates the infection probability between two records based on a given threshold of exposure duration. If the close contact time $R()$ is no shorter than the threshold, $f() = 100\%$; otherwise, $f() = 0\%$. As shown in an official report that the threshold for COVID-19 is 15 minutes [3], we set the threshold of exposure duration to be 15 minutes. Figure 14 reports the result.

We observe that, compared with the EC_{50} model, the numbers of finally infected passengers of all solutions are much higher. This is because the average travel time of bus trips is 826 seconds, which is close to the threshold. Roughly, almost half of contacts will cause a 100% infection ratio. It is worth noting that, even in this situation, CPT-SS still outperforms Top- k and Eig by an average of 50% and three times, respectively.

H. Scalability Study

In order to evaluate the performance of our solution CPT-SS in a different dataset, we conduct more experiments on a different EZ-link dataset with a ten times larger size from a different month. This dataset contains more than 13 million trip records. We also extend the prediction period from 14 days to 28 days to evaluate the scalability. Table VII shows the full experimental results, while Figure Figure 15 to 19 show a partial experimental results.

The result reported in Figure 15 shows the results of varying period. The longer periods is, the higher probability that we may suffer a pandemic. Figure 16 to 19 show the results of varying the number of checkpoints k in different incubation γ and infectious level EC_{50} . The results show that our solution consistently outperforms baselines by up to one order of

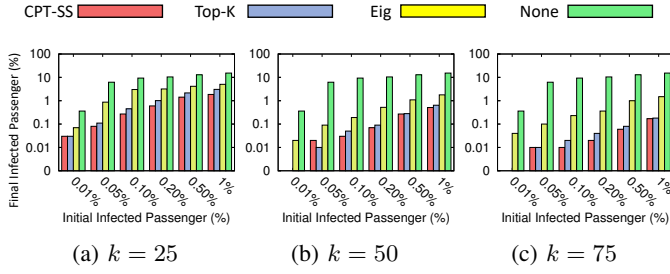


Fig. 18: Scalability - Varying k when $EC_{50} = 5400s$ and $\gamma = 72$ hours

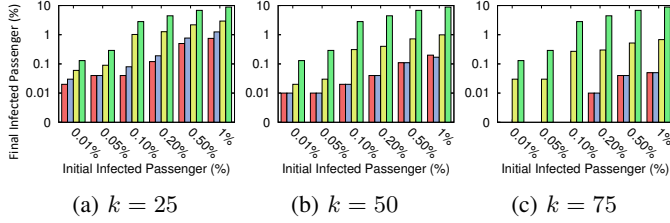


Fig. 19: Scalability - Varying k when $EC_{50} = 5400s$ and $\gamma = 120$ hours

magnitude. More specifically, compared with Top- k and Eig, the average advantages of our solution are around 40% and 350%, respectively. For the effectiveness, our method is able to finish with 10 minutes in all experiments.

We do not conduct the experiment when $EC_{50} = 1800$ second. In such a long period, a highly infectious virus will almost cause a pandemic, in which more than 90% passengers will be infected for all solutions. It is unrealistic and meaningless for compassion since the difference between each solution is small.

VIII. CONCLUSION

In this work, we study how to trace and mitigate virus diffusion according to fine-grained users' movement records. A critical challenge is how to capture the contact between mobile crowds to allow us to compute the infection probability based on the exposure duration. We first introduce a diffusion model based on TCG, which is able to exactly model the virus diffusion according to users' movements. Based on TCG, we propose *ESA* and *EMA* to assist governments to mitigate the epidemic from the defensive and offensive perspectives. In *EMA*, we aim to find an ideal checkpoint deployment strategy such that virus diffusion can be well mitigated. In *ESA*, we aim to find 'super-spreaders' to spread the virus maximally, in order to test deployment strategies. Finally, we conduct experiments using two real-world station datasets containing millions of public transport trip records to show that our TCG graph is able to evaluate the virus diffusion model more accurately compared with a snapshot-based dynamic graph. Moreover, in terms of finding a checkpoint deployment strategy, our solution outperforms the baselines over randomly infected passengers and super-spreaders under the varying infectious of viruses and different periods.

REFERENCES

- [1] W. H. Organization, "Managing epidemics: key facts about major deadly diseases," Tech. Rep., 2018.
- [2] —, "Advice on the use of masks in the context of covid-19," World Health Organization, Tech. Rep., 2020.
- [3] —, "Contact tracing in the context of covid-19," World Health Organization, Tech. Rep., 2020.
- [4] 7NEWS. (2020) Coronavirus china: Masked crowds fill streets and trains in post-lockdown wuhan. [Online]. Available: <https://7news.com.au/lifestyle/health-wellbeing/coronavirus-china-masked-crowds-fill-streets-and-trains-in-post-lockdown-wuhan-c-964849>
- [5] CNBC. (2020) Coronavirus: Photos of wuhan after 11-week lockdown. [Online]. Available: <https://www.cnbc.com/2020/04/08/wuhan-lifts-travel-restrictions-after-11-week-lockdown-see-photos.html>
- [6] T. W. Post. (2020) Some countries use temperature checks for coronavirus. [Online]. Available: https://www.washingtonpost.com/world/coronavirus-temperature-screening/2020/03/14/24185be0-6563-11ea-912d-d98032ec8e25_story.html
- [7] D. Chakrabarti, Y. Wang, C. Wang, J. Leskovec, and C. Faloutsos, "Epidemic thresholds in real networks," *ACM Trans. Inf. Syst. Secur.*, vol. 10, no. 4, pp. 1:1–1:26, 2008.
- [8] S. Chang, E. Pierson, P. W. Koh, J. Gerardin, B. Redbird, D. Grusky, and J. Leskovec, "Mobility network models of covid-19 explain inequities and inform reopening," *Nature*, pp. 1–8, 2020.
- [9] S. Ghamizi, R. Rwemalika, M. Cordy, L. Veiber, T. F. Bissyandé, M. Papadakis, J. Klein, and Y. L. Traon, "Data-driven simulation and optimization for covid-19 exit strategies," in *SIGMOD*, R. Gupta, Y. Liu, J. Tang, and B. A. Prakash, Eds. ACM, 2020, pp. 3434–3442.
- [10] Q. Hao, L. Chen, F. Xu, and Y. Li, "Understanding the urban pandemic spreading of COVID-19 with real world mobility data," in *SIGMOD*, R. Gupta, Y. Liu, J. Tang, and B. A. Prakash, Eds. ACM, 2020, pp. 3485–3492.
- [11] M. Minutoli, P. Sambaturu, M. Halappanavar, A. Tumeo, A. Kalyanaraman, and A. Vullikanti, "Preempt: scalable epidemic interventions using submodular optimization on multi-gpu systems," in *2020 SC20*. IEEE Computer Society, 2020, pp. 765–779.
- [12] Y. Chen, G. Paul, S. Havlin, F. Liljeros, and H. E. Stanley, "Finding a better immunization strategy," *Physical review letters*, vol. 101, no. 5, p. 058701, 2008.
- [13] P. Holme, B. J. Kim, C. N. Yoon, and S. K. Han, "Attack vulnerability of complex networks," *Physical review E*, vol. 65, no. 5, p. 056109, 2002.
- [14] C. M. Schneider, T. Mihaljev, S. Havlin, and H. J. Herrmann, "Suppressing epidemics with a limited amount of immunization units," *Physical Review E*, vol. 84, no. 6, p. 061911, 2011.
- [15] C. Chen, H. Tong, B. A. Prakash, T. Eliassi-Rad, M. Faloutsos, and C. Faloutsos, "Eigen-optimization on large graphs by edge manipulation," *ACM Trans. Knowl. Discov. Data*, vol. 10, no. 4, pp. 49:1–49:30, 2016.
- [16] B. A. Prakash, H. Tong, N. Valler, M. Faloutsos, and C. Faloutsos, "Virus propagation on time-varying networks: Theory and immunization algorithms," in *PKDD*, ser. Lecture Notes in Computer Science, J. L. Balcázar, F. Bonchi, A. Gionis, and M. Sebag, Eds., vol. 6323. Springer, 2010, pp. 99–114.
- [17] C. for Disease Control and P. (CDC), "Principles of epidemiology in public health practice," U.S. DEPARTMENT OF HEALTH AND HUMAN SERVICES, Tech. Rep., 2006.
- [18] K. Lin, D. Y.-T. Fong, B. Zhu, and J. Karlberg, "Environmental factors on the sars epidemic: air temperature, passage of time and multiplicative effect of hospital infection," *Epidemiology & Infection*, vol. 134, no. 2, pp. 223–230, 2006.
- [19] C. Nowzari, V. M. Preciado, and G. J. Pappas, "Analysis and control of epidemics: A survey of spreading processes on complex networks," *IEEE Control Systems Magazine*, vol. 36, no. 1, pp. 26–46, 2016.
- [20] R. M. Anderson, B. Anderson, and R. M. May, *Infectious diseases of humans: dynamics and control*. Oxford university press, 1992.
- [21] W. O. Kermack and A. G. McKendrick, "A contribution to the mathematical theory of epidemics," *Proceedings of the royal society of london. Series A, Containing papers of a mathematical and physical character*, vol. 115, no. 772, pp. 700–721, 1927.
- [22] H. W. Hethcote, "The mathematics of infectious diseases," *SIAM Rev.*, vol. 42, no. 4, pp. 599–653, 2000.
- [23] R. Pastor-Satorras, C. Castellano, P. Van Mieghem, and A. Vespignani,

- "Epidemic processes in complex networks," *Reviews of modern physics*, vol. 87, no. 3, p. 925, 2015.
- [24] J. Liu, P. E. Paré, A. Nedic, C. Y. Tang, C. L. Beck, and T. Basar, "Analysis and control of a continuous-time bi-virus model," *IEEE Trans. Autom. Control.*, vol. 64, no. 12, pp. 4891–4906, 2019. [Online]. Available: <https://doi.org/10.1109/TAC.2019.2898515>
- [25] S. Xu, W. Lu, L. Xu, and Z. Zhan, "Adaptive epidemic dynamics in networks: Thresholds and control," *ACM Trans. Auton. Adapt. Syst.*, vol. 8, no. 4, pp. 19:1–19:19, 2014. [Online]. Available: <https://doi.org/10.1145/2555613>
- [26] V. S. Mai, A. Battou, and K. Mills, "Distributed algorithm for suppressing epidemic spread in networks," *IEEE Control. Syst. Lett.*, vol. 2, no. 3, pp. 555–560, 2018. [Online]. Available: <https://doi.org/10.1109/LCSYS.2018.2844118>
- [27] V. M. Preciado, M. Zargham, C. Enyioha, A. Jadbabaie, and G. J. Pappas, "Optimal resource allocation for network protection against spreading processes," *IEEE Trans. Control. Netw. Syst.*, vol. 1, no. 1, pp. 99–108, 2014. [Online]. Available: <https://doi.org/10.1109/TCNS.2014.2310911>
- [28] S. Gracy, P. E. Paré, H. Sandberg, and K. H. Johansson, "Analysis and distributed control of periodic epidemic processes," *IEEE Trans. Control. Netw. Syst.*, vol. 8, no. 1, pp. 123–134, 2021. [Online]. Available: <https://doi.org/10.1109/TCNS.2020.3017717>
- [29] M. Nadini, K. Sun, E. Ubaldi, M. Starnini, A. Rizzo, and N. Perra, "Epidemic spreading in modular time-varying networks," *Scientific reports*, vol. 8, no. 1, pp. 1–11, 2018.
- [30] B. Wilder, S. Suen, and M. Tambe, "Preventing infectious disease in dynamic populations under uncertainty," in AAAI, S. A. McIlraith and K. Q. Weinberger, Eds. AAAI Press, 2018, pp. 841–848.
- [31] J. Zhan, T. Rafalski, G. Stashkevich, and E. Verenich, "Vaccination allocation in large dynamic networks," *Journal of Big Data*, vol. 4, no. 1, p. 2, 2017.
- [32] B. Liu, G. Cong, D. Xu, and Y. Zeng, "Time constrained influence maximization in social networks," in *ICDM*, M. J. Zaki, A. Siebes, J. X. Yu, B. Goethals, G. I. Webb, and X. Wu, Eds. IEEE Computer Society, 2012, pp. 439–448.
- [33] J. Kim, W. Lee, and H. Yu, "CT-IC: continuously activated and time-restricted independent cascade model for viral marketing," *Knowl. Based Syst.*, vol. 62, pp. 57–68, 2014.
- [34] S. Huang, Z. Bao, J. S. Culpepper, and B. Zhang, "Finding temporal influential users over evolving social networks," in *ICDE*. IEEE, 2019, pp. 398–409.
- [35] C. Ritz, F. Baty, J. C. Streibig, and D. Gerhard, "Dose-response analysis using r," *PloS one*, vol. 10, no. 12, p. e0146021, 2015.
- [36] P. Goyal and E. Ferrara, "Graph embedding techniques, applications, and performance: A survey," *Knowl. Based Syst.*, vol. 151, pp. 78–94, 2018.
- [37] J. Leskovec, J. M. Kleinberg, and C. Faloutsos, "Graph evolution: Densification and shrinking diameters," *ACM Trans. Knowl. Discov. Data*, vol. 1, no. 1, p. 2, 2007.
- [38] B. Gonçalves. (2020) Epidemic modeling 102: All covid-19 models are wrong, but some are useful. [Online]. Available: <https://medium.com/data-for-science/epidemic-modeling-102-all-covid-19-models-are-wrong-but-some-are-useful-c81202cc6ee9>
- [39] R. Li, S. Pei, B. Chen, Y. Song, T. Zhang, W. Yang, and J. Shaman, "Substantial undocumented infection facilitates the rapid dissemination of novel coronavirus (sars-cov-2)," *Science*, vol. 368, no. 6490, pp. 489–493, 2020. [Online]. Available: <https://science.sciencemag.org/content/368/6490/489>
- [40] J. A. Paulos. (2020) We're reading the coronavirus numbers wrong. [Online]. Available: <https://www.nytimes.com/2020/02/18/opinion/coronavirus-china-numbers.html>
- [41] F. Times. (2020) The mystery of the true coronavirus death rate. [Online]. Available: <https://www.ft.com/content/f3796baf-e4f0-4862-8887-d09c7f706553>
- [42] S. L. Wu, A. N. Mertens, Y. S. Crider, A. Nguyen, N. N. Pokpongkiat, S. Djajadi, A. Seth, M. S. Hsiang, J. M. Colford, A. Reingold *et al.*, "Substantial underestimation of sars-cov-2 infection in the united states," *Nature communications*, vol. 11, no. 1, pp. 1–10, 2020.
- [43] E. Garcia. (2020) New cutting-edge rapid test detects both covid-19 and flu. [Online]. Available: <https://health.ucdavis.edu/health-news/newsroom/new-cutting-edge-rapid-test-detects-both-covid-19-and-flu/2020/11>
- [44] G. Guglielmi. (2020) Fast coronavirus tests: what they can and can't do. [Online]. Available: <https://www.nature.com/articles/d41586-020-02661-2>
- [45] C. testing finally gathers speed. (2020) Cormac sheridan. [Online]. Available: <https://www.nature.com/articles/d41587-020-00021-z>
- [46] A. Logins, Y. Li, and P. Karras, "On the robustness of cascade diffusion under node attacks," in WWW, Y. Huang, I. King, T. Liu, and M. van Steen, Eds. ACM / IW3C2, 2020, pp. 2711–2717.
- [47] N. Ohsaka, T. Akiba, Y. Yoshida, and K. Kawarabayashi, "Dynamic influence analysis in evolving networks," *Proc. VLDB Endow.*, vol. 9, no. 12, pp. 1077–1088, 2016.
- [48] S. A. Vinterbo, "A note on the hardness of the k-ambiguity problem," *Technical Report DSG-T R-2002-006*, 2002.
- [49] C. Borgs, M. Brautbar, J. T. Chayes, and B. Lucier, "Maximizing social influence in nearly optimal time," in *SODA*, C. Chekuri, Ed. SIAM, 2014, pp. 946–957.
- [50] Q. Guo, S. Wang, Z. Wei, and M. Chen, "Influence maximization revisited: Efficient reverse reachable set generation with bound tightened," in *SIGMOD*, D. Maier, R. Pottinger, A. Doan, W. Tan, A. Alawini, and H. Q. Ngo, Eds. ACM, 2020, pp. 2167–2181.
- [51] Y. Tang, X. Xiao, and Y. Shi, "Influence maximization: near-optimal time complexity meets practical efficiency," in *SIGMOD*, C. E. Dyreson, F. Li, and M. T. Özsu, Eds. ACM, 2014, pp. 75–86.
- [52] X. Tian and B. Zheng, "Using smart card data to model commuters' responses upon unexpected train delays," in *IEEE Big Data*, 2018, pp. 831–840.
- [53] C. for Disease Control and P. (CDC), "Clinical signs and symptoms of influenza," U.S. DEPARTMENT OF HEALTH AND HUMAN SERVICES, Tech. Rep., 2020.
- [54] S. A. Lauer, K. H. Grantz, Q. Bi, F. K. Jones, Q. Zheng, H. R. Meredith, A. S. Azman, N. G. Reich, and J. Lessler, "The incubation period of coronavirus disease 2019 (covid-19) from publicly reported confirmed cases: estimation and application," *Annals of internal medicine*, vol. 172, no. 9, pp. 577–582, 2020.